

Lawrence Berkeley National Laboratory

Recent Work

Title

MEDICAL POSITRON IMAGING WITH A DESNE DRIFT SPACE MULTIWIRE PROPORTIONAL CHAMBER

Permalink

<https://escholarship.org/uc/item/6x31v6ms>

Author

Guerra, A. Del

Publication Date

1982-03-01



Lawrence Berkeley Laboratory

UNIVERSITY OF CALIFORNIA

Physics, Computer Science & Mathematics Division

Submitted to the Transaction on Medical Imaging

MEDICAL POSITRON IMAGING WITH A DENSE DRIFT
SPACE MULTIWIRED PROPORTIONAL CHAMBER

Alberto Del Guerra, Chun B. Lim, Gary K. Lum,
Douglas Ortendahl, and Victor Perez-Mendez

March 1982

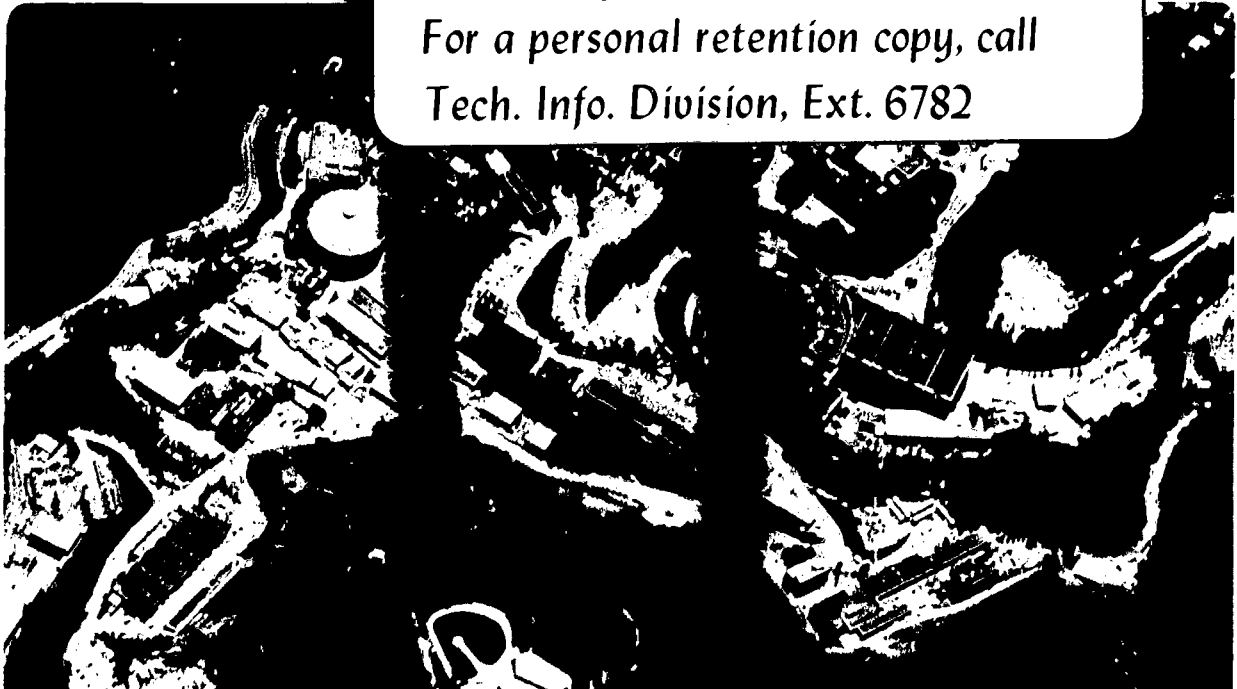
RECEIVED
LAWRENCE
BERKELEY LABORATORY

MAR 5 1982

LIBRARY AND
DOCUMENTS SECTION

TWO-WEEK LOAN COPY

*This is a Library Circulating Copy
which may be borrowed for two weeks.
For a personal retention copy, call
Tech. Info. Division, Ext. 6782*



LBL-14043
c.2

DISCLAIMER

This document was prepared as an account of work sponsored by the United States Government. While this document is believed to contain correct information, neither the United States Government nor any agency thereof, nor the Regents of the University of California, nor any of their employees, makes any warranty, express or implied, or assumes any legal responsibility for the accuracy, completeness, or usefulness of any information, apparatus, product, or process disclosed, or represents that its use would not infringe privately owned rights. Reference herein to any specific commercial product, process, or service by its trade name, trademark, manufacturer, or otherwise, does not necessarily constitute or imply its endorsement, recommendation, or favoring by the United States Government or any agency thereof, or the Regents of the University of California. The views and opinions of authors expressed herein do not necessarily state or reflect those of the United States Government or any agency thereof or the Regents of the University of California.

Medical positron imaging with a dense drift

space MultiWire Proportional Chamber+

Alberto Del Guerra*, Chun B. Lim⁽⁺⁾, Gary K. Lum**, Douglas Ortendahl⁽⁺⁺⁾,
and Victor Perez-Mendez

Lawrence Berkeley Laboratory, University of California, Berkeley, CA

Abstract

A multiplanar positron camera is proposed, made of six MWPC modules, arranged to form the lateral surface of a hexagonal prism. Each $50 \times 50 \text{ cm}^2$ module has a single MWPC sandwiched by two 2 cm thick lead glass tube converters. The experimental results for a $15 \times 15 \text{ cm}^2$ test module are reported. For 511 KeV γ -rays incident almost perpendicular onto a 1.0 cm thick converter, a detection efficiency of 4.3%, a time resolution of 130 ns (FWHM) and a spatial resolution of 2.8 mm (FWHM) has been measured with a standard Argon-Methane (70-30) mixture at 1.2 Atm. The chamber may be also operated in high resolution mode: 1.2 mm (FWHM) spatial resolution has been measured at a 50% lower efficiency. The use of fast delay lines (specific delay = 8 ns/cm) for the position read-out ensures a high rate capability. The expected performance of the six module MWPC camera is discussed and compared with that of BGO crystal ring camera. The MWPC solution seems very attractive not only for its low cost and simplicity of construction, but also for its fully three-dimensional imaging capability.

+ This work was supported by the Director, Office of Energy Research Office of High Energy and Nuclear Physics, Division of High Energy Physics of the US Department of Energy under Contract No. DE-AC03-76SF00098.

* On leave of absence from: Istituto di Fisica dell'Universita', Piazza Torricelli, 2, I-56100 Pisa, Italy.

** Present Address: Lockheed Missiles and Space Co., Inc., Sunnyvale, California.

+ Present Address: Siemens Gammasonics Inc., Illinois.

++ Present Address: University of California, Radiology Department, UCSF.

1. INTRODUCTION

Modern positron cameras are generally designed in two configurations: (a) single ring or multiring of many element scintillators, NaI⁽¹⁾ or BGO^(2,3) and more recently CsF,⁽⁴⁾ and (b) large area planar cameras of various types.

One of the main advantages of a large area multiplanar solution is its intrinsic capability of fully three-dimensional imaging. An example of multiplanar camera is sketched in Fig. 1: six modules, each a square of side ℓ , are arranged to form the lateral surface of an hexagonal prism. In a previous paper⁽⁵⁾ we have discussed the theory of tomographical imaging with limited angular input. Using such algorithms we may exploit the intrinsic multislice capability of our structure. On the x-y plane (Fig. 1b), a complete angle coverage is then obtained, because the few intermodule discontinuities are well accounted for by the limited angle reconstruction algorithms. On the perpendicular plane (Fig. 1c), a limited angle ($\sim 1/3$) is covered, but the limited angle reconstruction algorithms may successfully be used to recover the missing cone information⁽⁵⁾. Furthermore, due to its continuous structure, a multiplanar configuration does not require either wobbling⁽⁶⁾ or other mechanisms⁽⁷⁾ to provide a linear sampling; hence, many of the engineering complications of a ring structure may be avoided.

Among the various types of detectors which can be used in a large area multiplanar camera, the dense drift space MultiWire Proportional Chamber has been receiving a great amount of attention, both at Lawrence Berkeley Laboratory since 1973^(8,9) and, later, independently, at CERN^(10,11).

A well-known quality factor of a positron camera is ϵ^2/τ where ϵ is the efficiency of one element and τ is its time resolution (FWHM). In our case ϵ and τ are the efficiency and the time resolution of a MWPC module. We have previously reported⁽¹²⁾ the imaging performance of a two planar positron camera, consisting of two MWPC modules ($48 \times 48 \text{ cm}^2$ active area), equipped with converters made of lead corrugated band strips⁽¹³⁾. To increase the efficiency of the chamber we have subsequently developed lead glass tube converters⁽¹⁴⁾ with a higher surface to volume ratio. We have also investigated the most suitable gas mixture in order to optimize the factor ϵ^2/τ .⁽¹⁵⁾

In this paper the performance of a $15 \times 15 \text{ cm}^2$ MWPC test module with 1 cm thick lead glass tube converter is reported. The description of the experimental apparatus is given in section 2 and the experimental measurements on efficiency, time and spatial resolution are presented in section 3. Section 4 deals with the expected performance of the proposed six-module positron camera which is compared with that of recent BGO cameras. Finally some concluding remarks are given in the last section.

2. EXPERIMENTAL APPARATUS

We have built a $50 \times 50 \text{ cm}^2$ MWPC module, but, for convenience, we have extensively tested a smaller module, consisting of a MWPC ($15 \times 15 \text{ cm}^2$ active area), and 1 cm thick lead glass converter, both contained in an Aluminum box filled with the chosen gas mixture. In Fig. 2 we show a cross view of the test module (top) and a plan view of the MWPC (bottom). The anode plane is made of $20 \mu\text{m}$ stainless steel wires, spaced 3 mm apart, connected to a positive high voltage V_A , through a load protection resistor; the two

cathode planes consist of 100 μm stainless steel wires spaced 2 mm apart coupled through 220 $\text{k}\Omega$ resistors to a common bus bar. The anode-cathode gap is 5 mm. The directions of the wires in the cathode planes are arranged at 90° relative to each other in order to allow both x and y localization. The cathodes are kept at a positive voltage V_C relative to ground in order to drift the electrons out of the lead converter.

The detection of 511 KeV gamma rays requires the use of high density, high Z converter with large surface to volume ratio. We have developed a converter made of glass capillaries of high lead content (80% PbO by weight, glass density of 6.2 g/cm^3), fused to form honeycomb matrices. Details of the converter construction and treatment have been already reported⁽¹⁴⁾. Following the gamma interaction within the converter, the Compton - or photo-electron has a finite range depending on its energy. If it reaches the gas region within a tube, a number of primary ionization electrons are produced. A voltage difference, V_{conv} , applied between the ends of the tubes, then drifts these primary electrons along the electric field lines within the tube towards the cathode and into the avalanche region of the chamber.

X and Y position read-out is done by means of fast printed circuit delay lines (specific delay = 8 ns/cm) capacitively coupled to the cathode plane wires⁽¹⁶⁾. Standard integrated amplifiers and comparator electronics have been used. For each co-ordinate the signal from one end of the delay line is used as the START and the signal from the other end as the STOP of a Time to Amplitude Converter. A multi-channel analyzer is then used to obtain the time spectrum, which is directly related to the co-ordinate distribution.

Fig. 3 shows the experimental set-up. A positron emitting source ^{68}Ga is placed between a NaI scintillator and the MWPC module. The position

of the source relative to the NaI detector is such that a very small solid angle is subtended by the source at the converter plane ($\Delta\theta \sim 7^\circ$), thus avoiding any edge effect.

3. EXPERIMENTAL RESULTS

In a previous paper⁽¹⁵⁾, we have shown the results of efficiency measurements and electron transit time studies for various gas mixtures and tube diameters. The measurements reported in this section always refer to a 1 cm thick converter, inner diameter 0.91 mm, outer diameter 1.10 mm and a standard Argon - Methane (70-30) mixture at a pressure of 1.2 Atm. The cathode voltage V_c , has been kept at +400 V and the converter voltage, V_{conv} , at -400 V in order to maximize the electron drift velocity for our gas mixture⁽¹⁷⁾. Extrapolation to other gas mixtures and converters thicknesses may be easily performed combining these data with those of ref. (15). More details on the experimental measurements are reported elsewhere⁽¹⁸⁾.

The efficiency has been measured from the coincidence of the NaI signal with the MWPC anode signal (amplified 220 times). In Fig. 4 the efficiency as a function of the anode discriminator threshold is shown for two values of V_{eff} ($= V_A - V_c$). The data are corrected for the γ -absorption in the aluminum cover.

The amplitude spectrum of electrons produced by the 511 KeV γ interaction inside the converter is continuous. To have the maximum efficiency, the MWPC should detect any amount of primary ionization produced in the gas within the converter tubes. The arrows superimposed on the upper curve indicate the amplitudes of the signal produced by a primary ionization of 1, 2 and 5 electrons, when V_{eff} is 3350 V. They have been derived by linear interpolation from the signal produced by the X-rays of a ^{55}Fe source, considering that on average 200 ion pairs are produced by a 5.9 KeV

X-ray in Argon. However, these are conservative estimates, because at this voltage the MWPC is well inside the semi-proportional region. The anode discriminator threshold has been set at 30 mV (as also indicated by an arrow in Fig. 4), which is twice the electronic noise level and certainly below the two electron threshold at $V_{\text{eff}} = 3350$ V.

If the chamber is able to detect any amount of primary ionization produced within the tube, the efficiency of the module is only limited by the converter electron yield, i.e., by the probability of the conversion electrons to have enough energy to enter the gas region within the tube and to produce at least one ion-pair. In Table 1 the performance of our converter is compared with that of the converter developed by Jeavons⁽¹⁹⁾ at CERN. The γ interaction probability and the electron yield have been calculated using the EGS Monte Carlo code⁽²⁰⁾; the 200 KeV electron energy cut-off is chosen on the basis of previous analytical calculations^(8,10). The efficiency for 511 KeV γ -rays is shown for the same Argon-Isobutane mixture for both converters; the data of ref. (19) have been scaled down from the 662 KeV experimental value, according to ref. (10). In the last line of the table we show the converter "Q", i.e., the ratio between the measured efficiency and the γ interaction probability. The converter developed at CERN and the lead glass tube converter we used have basically the same performance ($Q \approx 0.3$); this might indicate that the maximum efficiency has been reached for converters with this packing fraction. Additional converters are now being assembled with smaller inner diameter tube in order to further improve the surface to volume ratio.

Time and spatial resolution measurements were taken with these standard voltage settings: $V_A = 3750$ V, $V_C = 400$ V, $V_{conv} = -400$ V, and the anode discriminator threshold set at 30 mV. Stable and reproducible conditions have been obtained over a six months period.

The efficiency measurements were done using a majority logic coincidence between a 260 ns NIM pulse from the NaI discriminator and a 20 ns NIM pulse from the MWPC anode discriminator. A typical time spectrum is shown in Fig. 5; the FWHM of this spectrum is 130 ns.

The spatial resolution along the y-direction (perpendicular to the anode wires) has been measured by collimating the ^{68}Ga source with a 2" thick lead variable slit. To enhance the signal to noise ratio, only the coincidence (NaI-MWPC) events were accepted. A typical spectrum for a 750 μm slit is presented in Fig 6.

Using the two ends of delay line technique, we have previously obtained a spatial resolution better than 150 μm (FWHM), when large pulses are produced from X-ray sources in a pressurized chamber⁽²¹⁾, and better than 400 μm (FWHM) at atmospheric pressure⁽²²⁾. In the present application the signals have an extremely large dynamic variation, both in amplitude (by more than two orders of magnitude) and in rise time. Because of the low specific delay, there is no appreciable distortion of the signal along the delay line; hence the timing error that may be introduced by the jitter is mostly cancelled out. However, to keep the maximum efficiency the threshold of the delay line comparator must be set at a very low level, comparable with the noise of the system, and a worse spatial resolution is achieved. As the comparator threshold is raised the efficiency diminishes, but spatial resolution improves. The bottom part of Fig. 6 shows the spatial resolution along the

y-coordinate as a function of the relative efficiency of the delay line. At a relative efficiency of 100%, 2.8 mm FWHM has been measured and ~2.3 mm (FWHM) at 70% relative efficiency. As the limit of the spatial resolution is reached (0.9 mm FWHM, i.e. the tube diameter), the relative efficiency has dropped to 30%. The measured spatial resolution along the x-coordinate is some 20% worse, due to the 3 mm spacing of the anode wires.

4. POSITRON CAMERA PERFORMANCE

Two main applications have been developed for dense drift space MWPC's positron camera. The first one is related to the study of angular correlation of positronium annihilation⁽²³⁾; in this case the counting rate is rather low and a slow (but dense) gas mixture can be used, such as Argon-Isobutane; the chamber may be operated in high resolution mode (0.9 mm FWHM). However, the most interesting application is medical imaging with positron emitters. In this latter case a fast gas must be used in order to diminish the transit time of the electron within the converter tube and thus to reduce the accidental coincidence rate; the spatial resolution measured with our test module, 2.8 mm, may be sufficient, because of the intrinsic resolution limits due to other factors, mainly to the positron range⁽²⁴⁾ and to the deviation from 180° emission of the two photons⁽²⁵⁾. Using these and previous experimental data⁽¹⁵⁾, and the experience achieved with an early version of a MWPC camera⁽¹²⁾, we proposed here a new positron camera for medical applications.

A schematic drawing of the camera is shown in Fig 7. Six modules, 50 x 50 cm² each, are arranged to form the lateral surface of an hexagonal prism. Each module consists of a standard MWPC chamber (2 mm spacing for both anode and cathode planes), with 2 cm thick converters on both sides. Fast

delay lines (8 ns/cm) will be used and a fast gas mixture⁽¹⁵⁾, such as 69% Ar + 20% CH₄ + 10% CF₄ + 1% C₂H₂. The expected efficiency is 15%, with a time resolution of 200 ns (FWHM). From the relation⁽¹²⁾

$$\epsilon^2/\tau = 8 \left[(\text{true coincidences})^2 / \text{accidentals} \right],$$

assuming the true coincidence and accidental rates to be the same, we obtain a true coincidence rate of 14000 c/sec. In table 2 the performance of the proposed camera is compared with that of the previous one⁽¹²⁾.

In table 3 we show a comparison between the performance of the MWPC camera and two recent Bismuth Germanate ring cameras: the Donner single ring 280-BGO-crystal Positron Tomograph⁽²⁾ and the multiring NIH-Neuro PET⁽²⁶⁾. The latter was specifically designed as a high spatial resolution camera for brain imaging. The efficiency and the time resolution of the MWPC solution are still less favorable than the BGO case, but the spatial resolution is much higher. It has been shown⁽²⁷⁾ that the reconstruction image when the detector has 2 mm spatial resolution is of the same quality (in terms of signal to noise ratio) of that obtained with a 10 mm spatial resolution detector but with ten times more statistics. This means that the higher spatial resolution of a MWPC partially compensates its reduced efficiency. Furthermore, the MWPC positron camera has an intrinsic multislice capability, whereas the Donner Tomograph has none and Neuro PET can only produce four simultaneous intraring slices. The MWPC solution, in fact, is characterized by a fully three-dimensional imaging capability, with the voxel (volume element) size determined by the detector resolution. For a 15 x 15 x 15 cm³ phantom and for the proposed camera, as many as fifty (3 mm) independent slices can be simultaneously obtained.

Further work is now in progress to simulate the performance of such a camera for a point-like source embedded in a 20 cm diameter water phantom. The EGS code⁽²⁰⁾ will be used, which has been already applied to study low energy photon Compton scattering in medical imaging⁽²⁸⁾. The Monte Carlo data will then be reconstructed using limited angle algorithms⁽⁵⁾. The results of the simulation and the calculated sensitivity per slice (3 mm apart) and for the whole system will be presented in a forthcoming paper.

5. CONCLUSIONS

We have studied the performance of a dense drift space MWPC test module for 511 KeV γ -rays. We have measured the three characteristic parameters: efficiency (4.3%), time resolution (130 ns FWHM) and spatial resolution (2.8 mm FWHM). We have also discussed how important it is to measure these three parameters in the same experimental conditions; nonetheless, applications may be envisaged where one parameter has more relevance than the others.

A six module MWPC positron camera has been proposed, as a high spatial resolution camera for medical imaging with positron emitters. Its expected performance is compared with those of two different BGO cameras and is shown to be very competitive.

The progress in electronics technology and the increased knowledge of gas properties has now rendered the MWPC camera very attractive, not only for its low cost and simplicity of construction, but also because of the large solid angle coverage and the high spatial resolution. Its intrinsic three-dimensional (multislice) capability makes this solution competitive with the recently proposed, but much more expensive, spherical scintillator camera⁽²⁹⁾.

The assistance of P. Wiedenbeck in drawing the figures is greatly acknowledged.

REFERENCES

1. N.A. Mullani, M.M. Ter-Pogossian, C.S. Higgings, J.T. Hood, and D.C. Ficke, "Engineering aspects of PETT V", IEEE Trans. Nucl. Sci., Vol. NS-26, pp 2703-2706, 1979.

L. Eriksson, Chr. Bohm, M. Bergstrom, K. Ericson, T. Greitz, J. Litton, and L. Widen, "One year experience with a high resolution ring - detector positron camera system: present status and future plans", IEEE Trans. Nucl. Sci., Vol. NS-27, pp 435-444, February 1980.
2. S.E. Derenzo, T.F. Budinger, R.H. Huesman, J.L. Cahoon and T. Vuletich, "Imaging properties of a Positron Tomograph with 280 BGO crystals", IEEE Trans. Nucl. Sci., Vol. NS-28, pp. 81-89, February 1981.
3. E. Hoffman, M. Phelps, S. Huang, D. Plummer and D. Kuhl, "Performance characteristics of a Multi-plane Positron Tomograph designed for Brain Imaging", IEEE Trans. Nucl. Sci., Vol. NS-29, No. 1, February 1982, in press.

L. Eriksson, Chr. Bohm, G. Blomquist, J. Litton, and L. Widen, "A Four Ring Positron Camera System for Emission Tomography of the Brain", IEEE Trans. Nucl. Sci., Vol. NS-29, No. 1, February 1982, in press.
4. R. Allemand, C. Gresset, and J. Vacher, "Potential advantages of a Cesium Fluoride Scintillator for a time-of-flight positron camera", J. Nucl. Med., Vol 21, pp 153-155, 1980.

D. Ficke, D. Beecher, G. Hoffman, J. Hood, J. Markham, N. Mullani, and M. Ter-Pogossian, "Engineering Aspects of PETT VI", IEEE Trans. Nucl. Sci., Vol. NS-29, No. 1, February 1982, in press.

M. Yamamoto, D.C. Ficke, M. Ter-Pogossian, "Performance study of PETT VI, a Positron computed Tomograph with 288 Cesium Fluoride Detectors", IEEE Trans. Nucl. Sci., Vol. NS-29, No. 1, February 1982, in press.
5. K.C. Tam and V. Perez-Mendez, "Tomographical imaging with limited-angle input", J. Opt. Soc. Am., Vol. 71, pp. 582-592, 1981.
6. R.A. Brooks, V.J. Sank, A.J. Talbert, and G. Di Chiro, "Sampling requirements and detector motion for positron emission Tomography", IEEE Trans. Nucl. Sci., Vol. NS-26, pp. 2760-2763, 1979.
7. S.E. Derenzo, "Detectors, sampling, shielding and Electronics for Positron Emission Tomography", Lawrence Berkeley Laboratory, LBL-13091 (1981) and to be published in Trans. Am. Nucl. Soc. (1982).

8. C.B. Lim, D. Chu, L. Kaufman, V. Perez-Mendez and J. Sperinde, "Characteristics of Multiwire Proportional Chambers for Positron Imaging", IEEE Trans., Nucl. Sci., Vol. NS-21, pp. 85-88, February 1974.
9. C.B. Lim, D. Chu, L. Kaufman, V. Perez-Mendez, R. Hattner, and D.C. Price, "Initial Characterization of a Multi-Wire Proportional Chamber Positron Camera", IEEE Trans. Nucl. Sci. Vol, NS-22, pp. 388-394, February 1975.
10. A.P. Jeavons, G. Charpak and R.J. Stubbs, "The High-Density Multiwire Drift Chamber", Nucl. Instr. and Meth., Vol. 124, pp. 491-503, 1975.
11. A.P. Jeavons, "The High-Density Proportional Chamber and its Applications", Nucl. Instr. and Meth., Vol. 156, pp. 41-51, 1978.
12. V. Perez-Mendez, C.B. Lim, D. Ortendhal, R. Semper, A. Cheng, D. Chu, R. Hattner, L. Kaufman and D.C. Price, "Two detector MWPC Positron camera with honeycomb lead converters for medical imaging: performance and developments", Nucl. Instr. Meth., Vol. 156, pp. 33-40, 1978.
13. D. Chu, K.C. Tam, V. Perez-Mendez, C.B. Lim, D. Lambert, and S.N. Kaplan, "High Efficiency Collimator-Converters for Neutral Particle Imaging With MWPC", IEEE Trans. Nucl. Sci., Vol. NS-23, pp. 634-639, February 1976.
14. G.K. Lum, M.I. Green, V. Perez-Mendez and K.C. Tam, "Lead Oxide Glass Tubing Converters for Gamma Detection in MWPC", IEEE Trans. Nucl. Sci., Vol. NS-27, pp. 157-165, February 1980.
G.K. Lum, D. Anderberg, M.I. Green, P. Henrickson, and V. Perez-Mendez, "The Development of High Density PbO Macrochannel Plates for High Energy Gamma-Ray Detection", Proceedings 25th American Scientific Glassblowers Society Symposium, Albany, N.Y., June 25-27, 1980.
15. G.K. Lum, V. Perez-Mendez, and B. Sleaford, "Gamma-Ray Detection with PbO Glass Converters in MWPC: Electron Conversion Efficiency and Time Resolution", IEEE Trans. Nucl. Sci., Vol. NS-28, pp. 821-824, February 1981.
16. P. Lecomte, V. Perez-Mendez and G. Stoker, "Electromagnetic Delay Lines in Spark Proportional and Drift Chamber Applications", Nucl. Instr. and Meth., Vol. 153, pp. 543-551, 1978.
17. B. Jean-Marie, V. Lepeltier, and D. L'Hote, "Systematic Measurement of electron drift velocity and study of some properties of four gas mixtures: A-CH₄, A-C₂H₂, A-C₂H₆, A-C₃H₈", Nucl. Instr. Meth., Vol 159, pp. 213-219, 1979.
18. A. Del Guerra, G.K. Lum, V. Perez-Mendez, G. Schwartz, "High Spatial resolution MWPC for medical imaging with positron emitters", Lawrence Berkeley Laboratory LBL-14044, to be submitted to Nucl. Instr. and Meth., 1982.

19. A. Jeavons, K. Kull, B. Lindberg, G. Lee, D. Townsend, P. Frey and A. Donath, "A Proportional Chamber Positron Camera for Medical Imaging", Nucl. Instr. and Meth., Vol. 176, pp. 89-97, 1980.
20. R.L. Ford and W.R. Nelson, "The EGS code system: Computer program for the Monte Carlo Simulation of Electromagnetic Cascade Showers (Version 3)", Stanford Linear Accelerator Center, SLAC-210, June 1978.
21. A.R. Forouhi, B. Sleaford, V. Perez-Mendez, D. de Fontaine, and J. Fodor, "Small-Angle X ray Scattering system with linear position - sensitive detector", IEEE Trans. Nucl. Sci., Vol. NS-29, No. 1, February 1982, in press.
22. R. Bellazzini, G. Betti, A. Del Guerra, M.M. Massai, M. Ragadini, G. Spandre, G. Tonelli and R. Venturi, "Electronic autoradiography of Human living cells with a MWPC", to be published in Nucl. Instr. and Meth., 1982.
23. A.A. Manuel, S. Samoilov, O. Fischer and M. Peter, "The use of High Density Proportional Chambers for Positron Annihilation Studies in Aluminum, Copper, and V_3Si ", in Proc. 5th Int. Conf. on Positron Annihilation, Sendai, Japan, pp. 685-694, 1979.
24. S. Derenzo, "Precision Measurement of annihilation point spread distribution for medically important positron emitters", in Proc. 5th Int. Conf. on Positron Annihilation, Sendai, Japan, pp. 819-823, 1979.
25. P. Colombino, B. Fiscella, and L. Trossi, "Study of positronium in water and ice from 22 to $-144^{\circ}C$ by annihilation quanta measurements", Nuovo Cimento, Vol. 38, pp. 707-723, 1965.
26. R.A. Brooks, V.J. Sank, W.S. Friauf, S.B. Leighton, H.E. Cascio and G. Di Chiro, "Design Considerations for Positron Emission Tomography", IEEE Trans. Biom. Eng., Vol. BME-28, pp. 158-177, February 1981.
27. M.E. Phelps, in "Workshop on Positron Emission Tomography", IEEE 1981 Nuclear Science Symposium, IEEE Trans. Nucl. Sci., Vol NS-29, No. 1, February 1982, in press.
28. A. Del Guerra, R. Bellazzini, G. Tonelli, R. Venturi and W.R. Nelson, "A detailed Monte Carlo Study of multiple scattering contamination in Compton tomography at 90 degrees", Lawrence Berkeley Laboratory, LBL-14045, and submitted to IEEE Trans. Med. Imag., 1982.
29. Z.H. Cho, K.S. Hong, J.B. Ra, S.K. Hilal, and J. Correll, "High Resolution, Spherical Positron Emission Tomography (S-PET) and its Design Analysis", IEEE Trans. Nucl. Sci., Vol. NS-29, No. 1, February 1982, in press.

TABLE 1. CONVERTER PERFORMANCE

	Jeavons et al. (19)	This work
Converter type	Stack of perforated metal plates (0.1 mm thick) interspaced with (0.1 mm thick) fiberglass plates.	Lead glass tubes fused to form a honeycomb matrix
Inner diameter (mm)	0.8	0.91
Outer diameter (mm)	1.0	1.10
High Z component	Pb-Sn-Sb (96%-2%-2%)	PbO (80%)
Total thickness (cm)	0.96	1.0
Interaction Probability for 511 KeV γ -rays ($\times 10^2$)	27.7	20.7
Yield of electrons with an energy greater than 200 KeV ($\times 10^2$)	22.0	15.2
Efficiency of the chamber with Argon-Isobutane mixture for 511 KeV γ -rays ($\times 10^2$)	6.8*	6.2 ⁺
Efficiency/ γ Interaction probability ("Q" of the converter)	0.25	0.30

(*) Scaled down from the measured efficiency at 662 keV according to ref. (10).

(+) From combined measurements of this work and of ref. (15).

TABLE 2. POSITRON CAMERA SPECIFICATIONS AND PERFORMANCE

	Previous work (12)	This paper
Number of modules (= planes)	2	6
Solid angle fraction coverage	0.33	~0.50
Camera inner diameter	45 cm	85 cm
Active area of each module	48 x 48 cm ²	45 x 45 cm ²
Angular acceptance of each module pair	±40°	± 30°
Number of converters per module	3(*)	2
Converter type	Lead corrugated band strips	Lead glass tube honeycomb matrix
Position read-out system	Helical phase compensated slow delay lines	Printed circuit fast delay lines
Total delay of the delay line	1.2 μs	400 ns
Efficiency of each module	0.058	0.15
Time resolution (FWHM)	300 ns	200 ns
ϵ^2/τ (in unit x 10 ³ sec ⁻¹)	12	112
Point response function (in air)	7 mm	~2 mm
Operating counting rate (true coincidences = accidentals)	500 c/s	28000 c/s
Reconstruction algorithms	Back projection	Limited angle

(*) Each module had two MWPC's: the front one had two converters and the back MWPC only one converter.

TABLE 3. HIGH-SPATIAL RESOLUTION CAMERAS PERFORMANCE

	Donner Lab Positron Tomograph(2)	NIH Neuro PET (26)	This work
Type	Single Ring of BGO Scintillator	Multi-ring of BGO Scintillator	Dense Drift Space MWPC
Inner Diameter	94 cm	38 cm	85 cm
Number of ele- ment	280	128	6
Active volume of each element	$9.5 \times 32 \times 32 \text{ mm}^3$	$8.5 \times 20 \times 35 \text{ mm}^2$	$450 \times 450 \times 70 \text{ mm}^2$
Threshold	250 KeV	255 KeV ⁺	~200 KeV*
Time Resolu- tion (FWHM)	15 ns	20 ns	200 ns
Detection Efficiency	0.67	~0.70 ⁺	0.15
Point Response function in air	7 mm	4.6 mm	~2.0 mm**
Multislice capability	No	Yes	Yes
Number of con- temporary slices	1 (~1 cm slice)	4 (~1 cm slice)	50 (3 mm slice)

(+) In high sensitivity mode.

(*) Based on the intrinsic low sensitivity of the dense drift MWPC to photons with energy less than 200 KeV.

(**) A spatial resolution of 1.5 mm has been measured with the test module pressurized at 2 Atm (18).

(***) Based on a 27 mm^3 voxel and a $15 \times 15 \times 15 \text{ cm}^3$ object.

FIGURE CAPTIONS

1. An hexagonal-type multiplanar positron camera: a) perspective view, b) plan view, c) cross view.
2. Test chamber with the converter at the bottom separated from the cathode plane by a 4 mm spacing (top). Plan view of the chamber showing the orientation of the cathode planes with the delay lines coupled to them; the anode wires are also indicated by dashed lines (bottom).
3. Experimental set-up used to measure the efficiency, the time and spatial resolution of our test chamber to 511 KeV gamma rays (figure not to scale).
4. Efficiency of the chamber as a function of the anode discriminator threshold for two different effective voltages: a) solid circles data refer to Anode-Cathode voltage of 3350 V; b) open square data to the lower voltage of 3150 V.
5. Typical time distribution spectrum as obtained from the coincidence with the NaI scintillator. The FWHM of the distribution is 130 ns (Hor. scale = 50 ns/div). The start of the 280 ns coincidence gate is also shown.
6. Typical spatial resolution spectrum obtained with a 750 μm slit. The FWHM of the distribution is 37 channels corresponding to ~ 2.5 mm (top). Variation of the spatial resolution (FWHM) with the relative efficiency of the delay line (bottom). The minimum value of 0.9 mm corresponds to the inner diameter of the collimator tube.
7. Proposed Positron Camera of six modules arranged to form an hexagonal prism. Each module has a $45 \times 45 \text{ cm}^2$ active area and has two 2 cm thick lead glass tube converters.

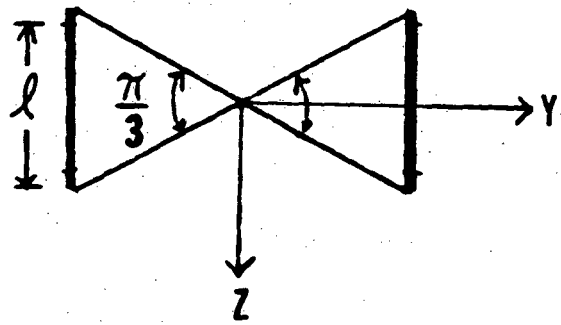
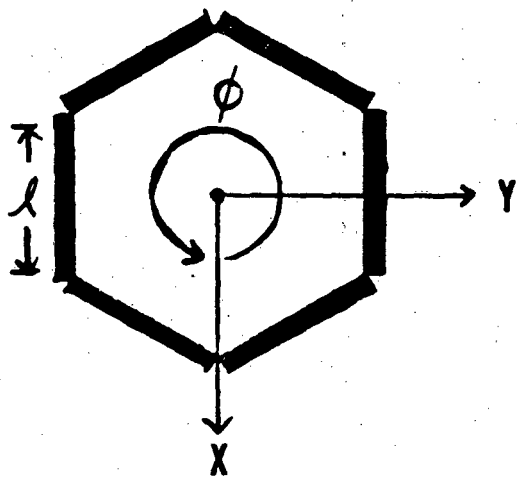
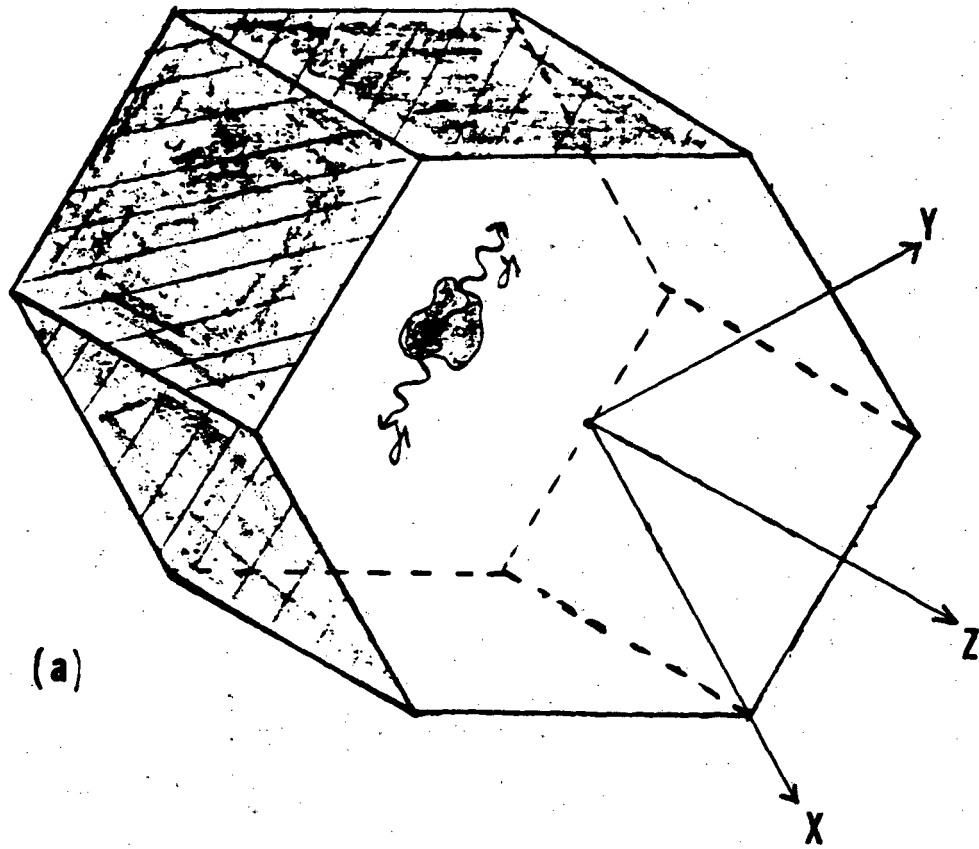
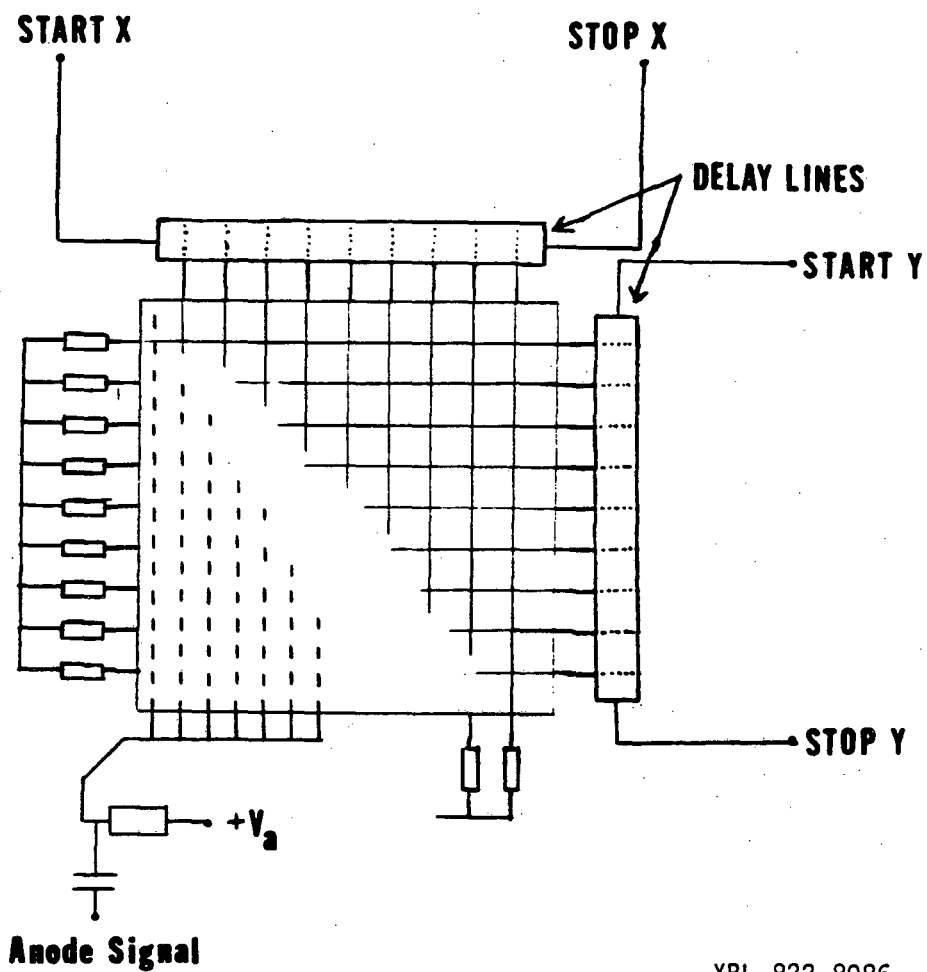
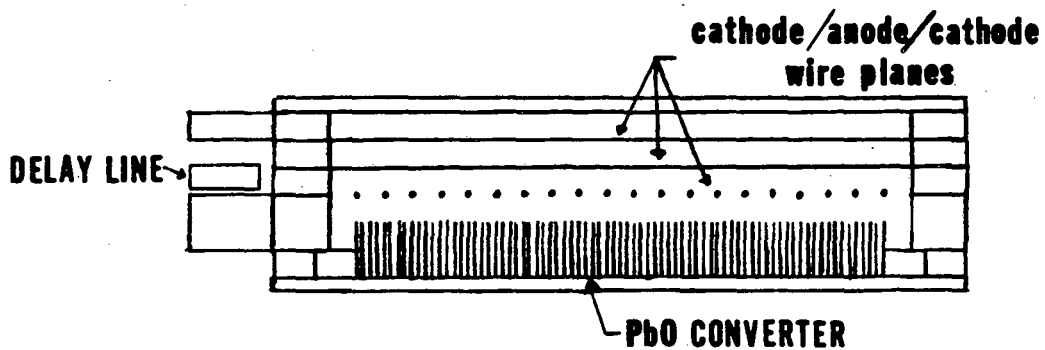


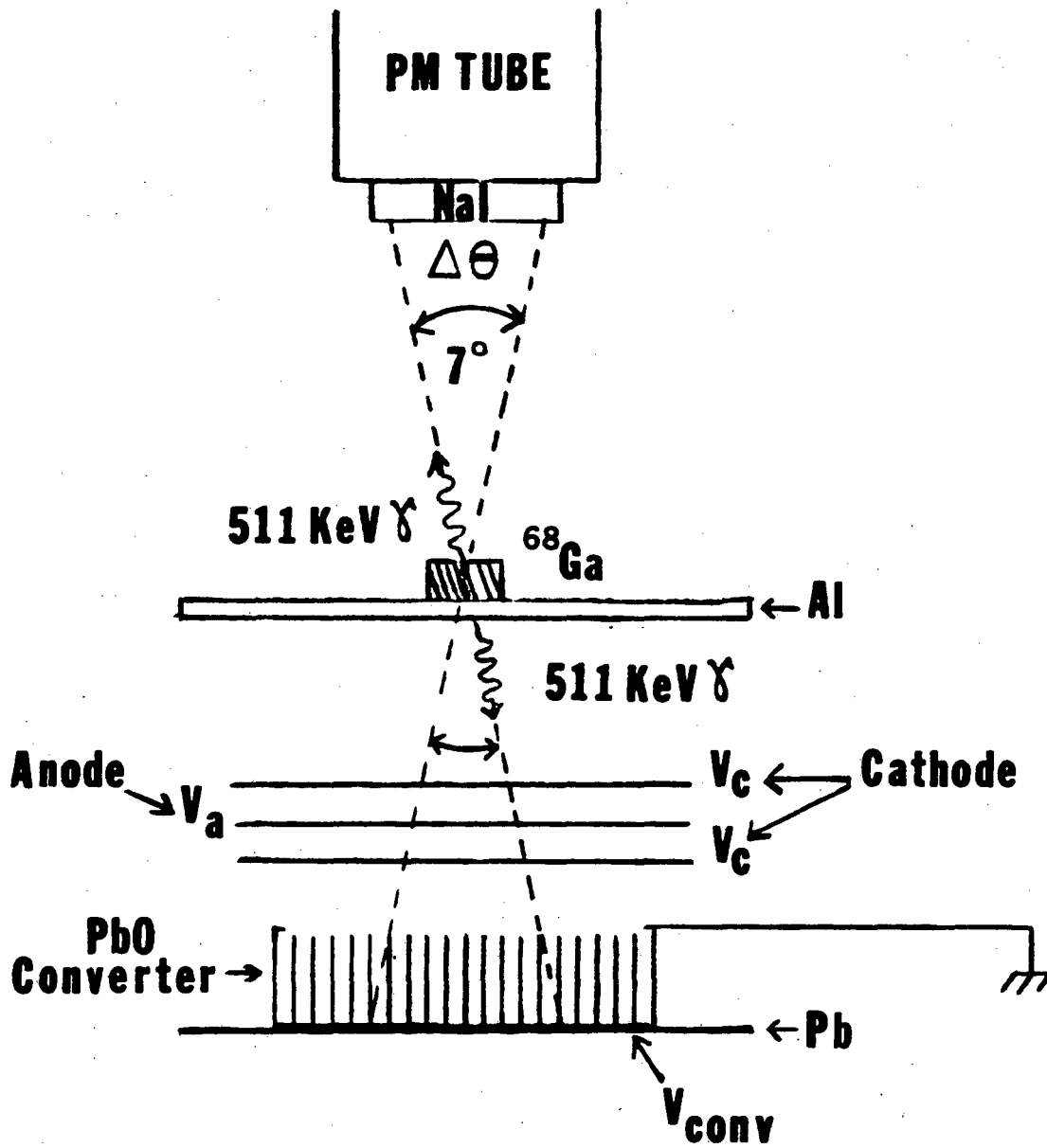
Fig. 1

XBL 822-8090



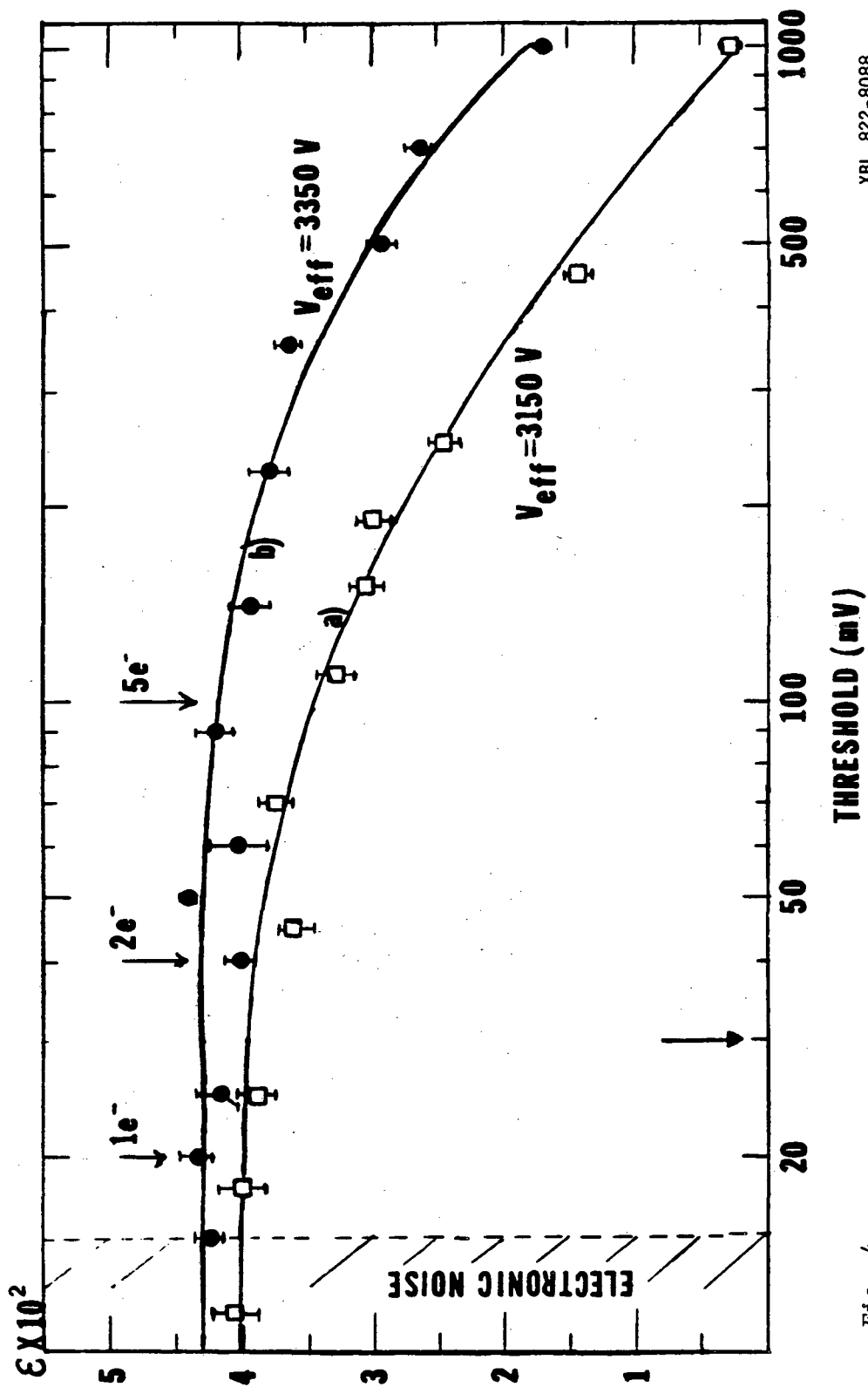
XBL 822-8086

Fig. 2



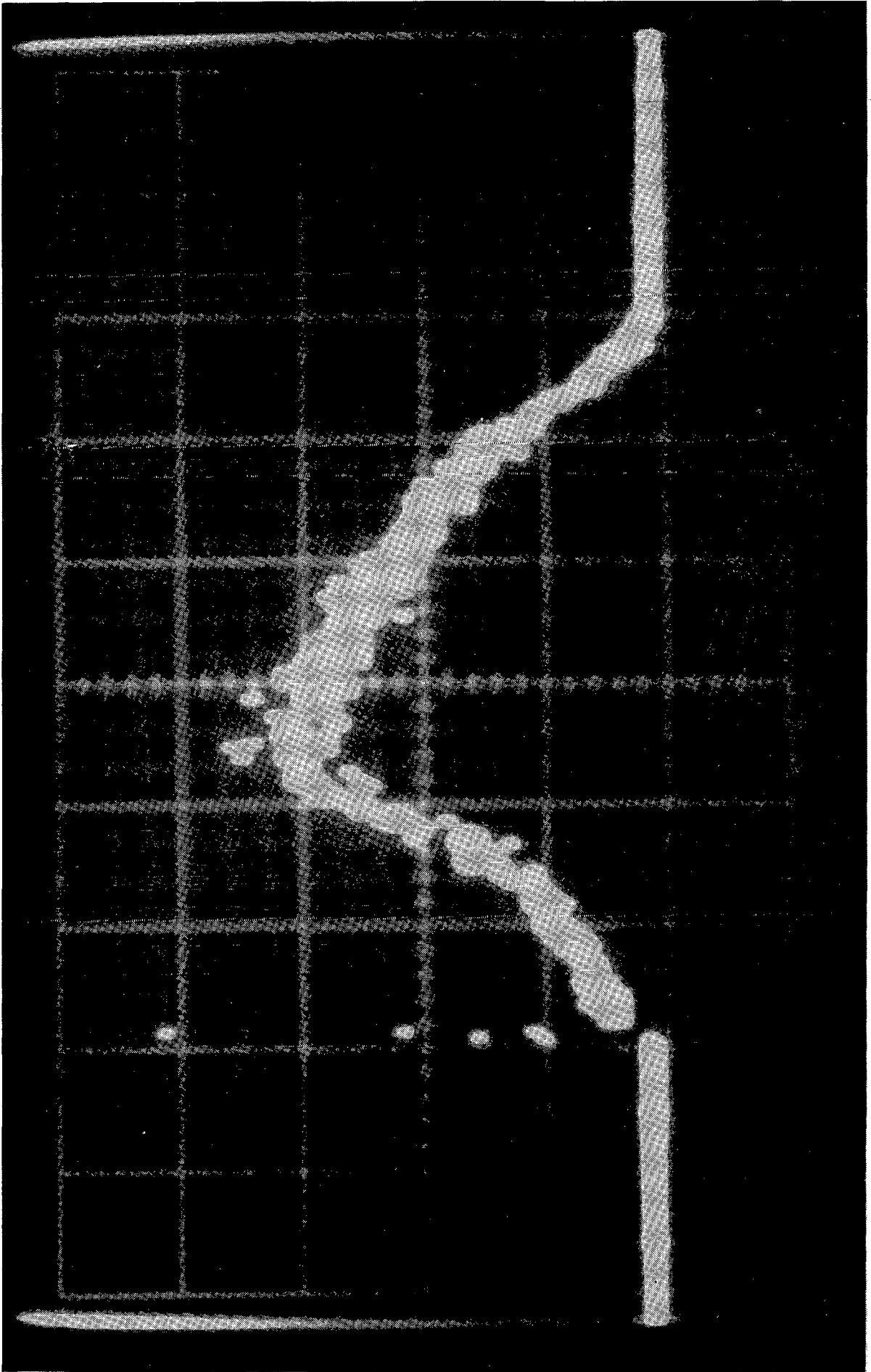
XBL 822-8087

Fig. 3



XBL 822-8088

Fig. 4



XBB 822-1481

Fig. 5

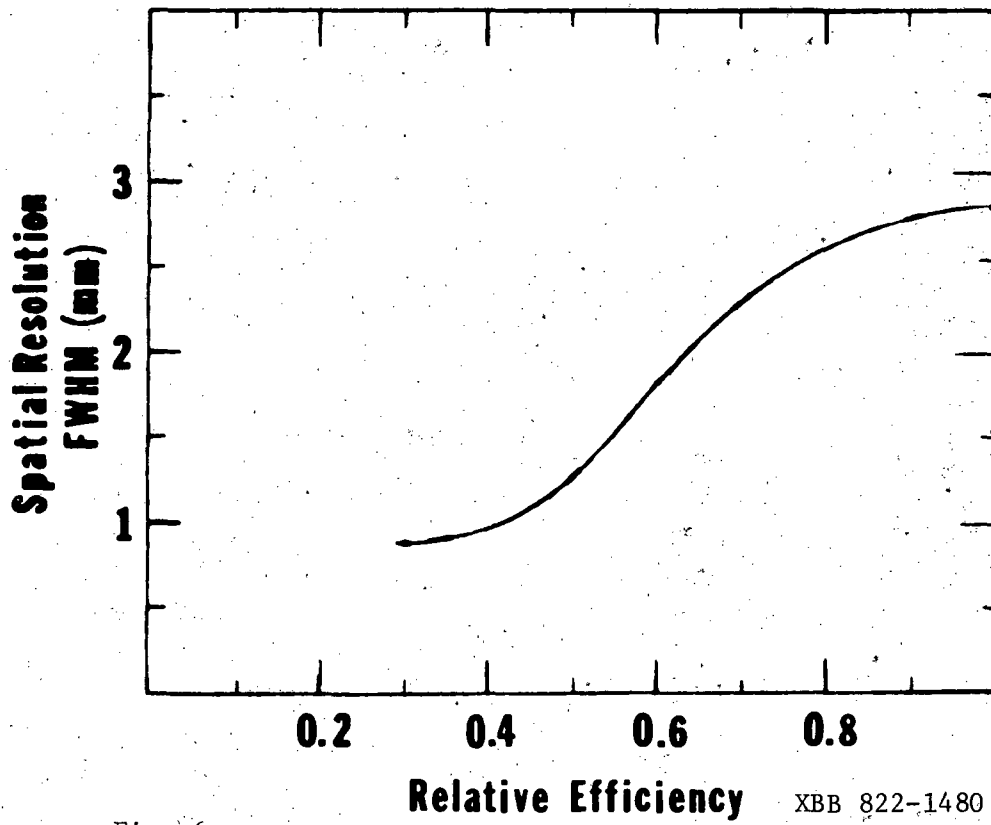
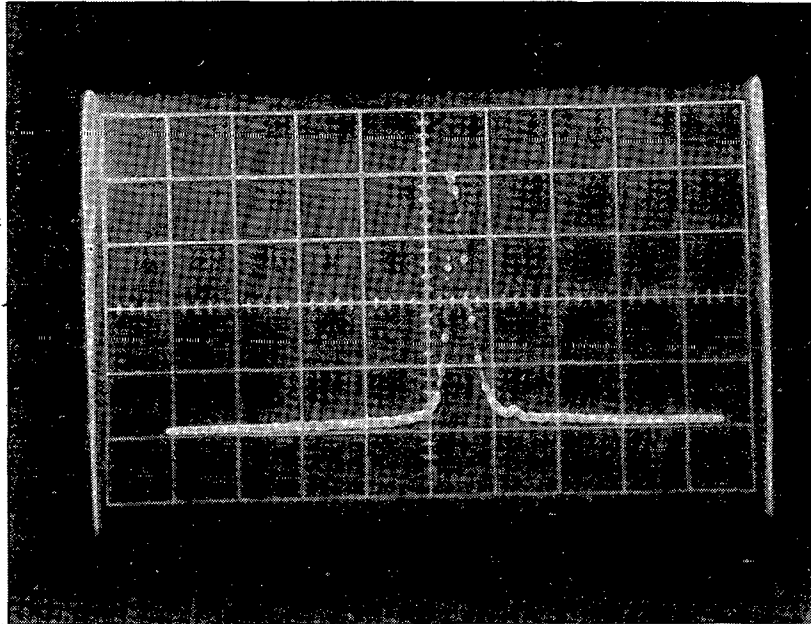
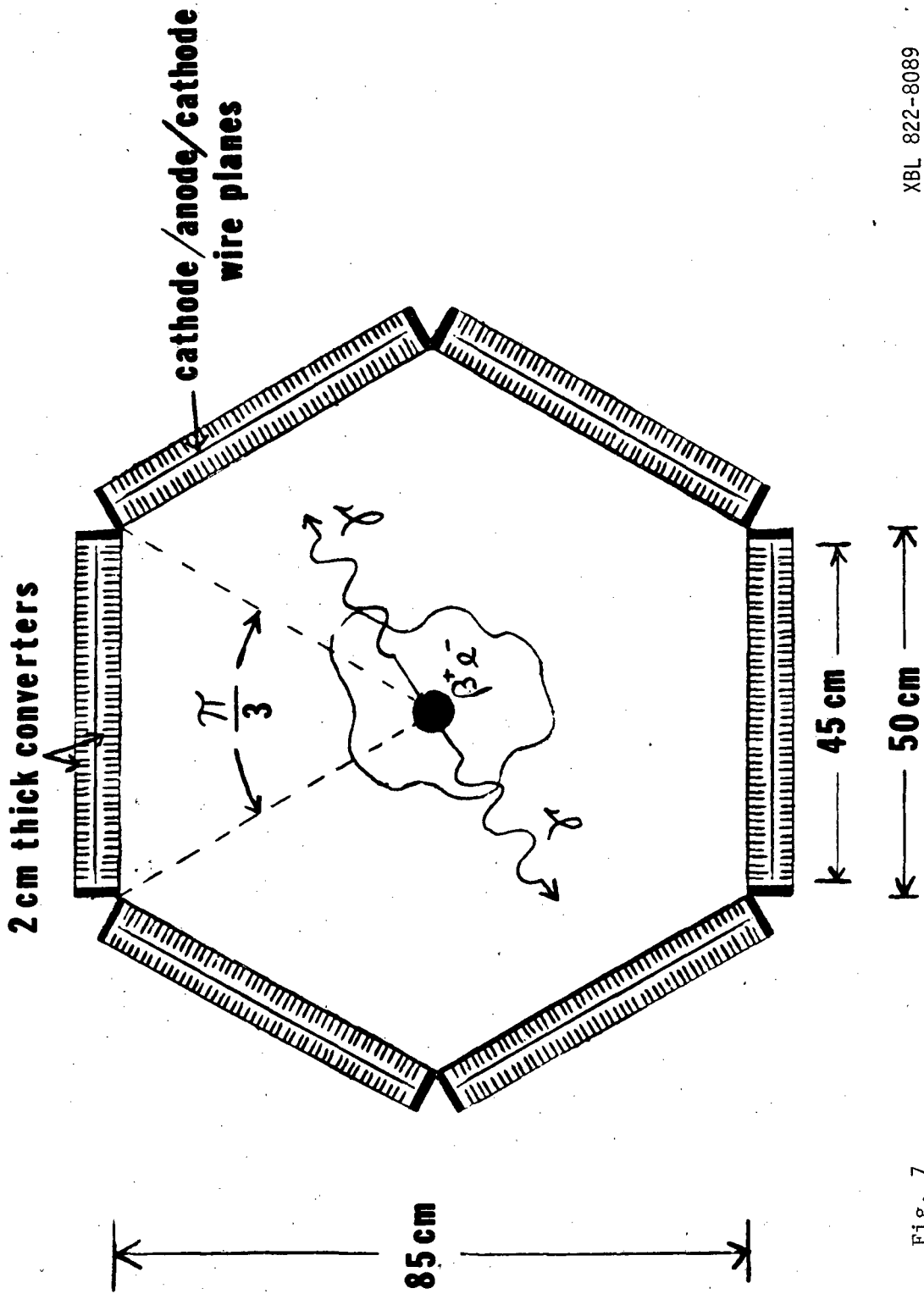


Fig. 6

XBB 822-1480



XBL 822-8089

Fig. 7

This report was done with support from the Department of Energy. Any conclusions or opinions expressed in this report represent solely those of the author(s) and not necessarily those of The Regents of the University of California, the Lawrence Berkeley Laboratory or the Department of Energy.

Reference to a company or product name does not imply approval or recommendation of the product by the University of California or the U.S. Department of Energy to the exclusion of others that may be suitable.

TECHNICAL INFORMATION DEPARTMENT
LAWRENCE BERKELEY LABORATORY
UNIVERSITY OF CALIFORNIA
BERKELEY, CALIFORNIA 94720